



A Fully Quantum Mechanical Theory of Radiation Damping and the Free-induction Decay in Magnetic Resonance

James S. Tropp

Berkshire Magnetics LLC, Berkeley, CA, USA

For most of its history, magnetic resonance has been described semiclassically, with spins treated by quantum mechanics and magnetic fields by classical physics. Here, we use the formalism of cavity quantum electrodynamics to give a fully quantum mechanical theory. We do not quantize the RF field directly but, instead, couple the spins to a quantized harmonic oscillator, representing the probe. This enables accurate numerical estimates of the rate of radiation damping in NMR. To facilitate these calculations, we also present a new semiclassical theory of radiation damping, rewritten using the reciprocity theory to eliminate the filling factor. Throughout we emphasize that radiation damping, usually considered a nuisance by practitioners, forms the basis for signal reception and occurs in every magnetic resonance experiment.

Keywords: cavity quantum electrodynamics, quantized LC oscillator, quantum Bloch vector, photons, coherence

How to cite this article:

eMagRes, 2016, Vol 5: 1077–1086. DOI 10.1002/9780470034590.emrstm1495

Introduction

The fundamental process of signal reception in NMR is the transfer of a photon from the nuclear spin system to the detector, typically a tuned RF coil. This loss of Zeeman energy by the spins causes the precessing nuclear moment to tilt slightly toward the vertical; when this process is fast relative to transverse relaxation (or other decay mechanisms), it causes unwanted broadening of the spectroscopic line, and has therefore received the name of radiation damping. Usually regarded as an occasional nuisance when observing strong signals, radiation damping is in fact present in every NMR experiment, and constitutes the means by which a detectable signal is formed. Taking the common case of a coil perfectly impedance matched to the receiver, half of the energy gotten from the spins is sent to the preamplifier (i.e., radiated), while the other half is lost in the coil's own resistance.

Given that NMR is a mature discipline, with widespread application in fields as diverse as chemical physics and clinical medicine, it is surprising that a satisfactory quantum mechanical theory of damping was not given early on, particularly since quantum optics offers a model – that of Jaynes and Cummings¹ – which is well adapted to the description of NMR, and has been recently employed for that purpose by the present author.² Jaynes and Cummings studied the ammonia maser, but their theory applies to any two-level atom – or spin $1/2$ – coupled to a quantized cavity; and their work can be considered the cornerstone of cavity quantum electrodynamics (CQED), a field^{3,4} for which a Nobel prize was awarded in 2012. Although Jaynes and Cummings dealt with electric fields and dipole moments, we shall describe their work in terms of the corresponding magnetic quantities.

But a workable quantum theory of radiation damping also requires reexamination of the semiclassical theory, first proposed in the seminal paper⁵ of Bloembergen and Pound (B–P) and reused, largely without modification, over the ensuing half-century. In fact, the semiclassical approach – with spins treated by quantum mechanics, and electrical entities, for example, cavities, fields, and antennas, by classical physics – has been dominant throughout the history of NMR. In what follows, we counter that tendency, and use pure quantum mechanics, via the Jaynes–Cummings model, to illustrate in fine detail the mechanism of signal formation in NMR; we also introduce a new semiclassical theory of radiation damping (rewritten to eliminate the troublesome filling factor) which, combined with the J–C model, enables quantitative calculation by quantum mechanics of the signal strength in NMR. Along the way we encounter certain counterintuitive results, well known in CQED, such as the nonclassical behavior of the quantum Bloch vector.² These pertain to the ongoing work, shared by CQED and NMR, of formulating the transition between the fully quantum mechanical and the semiclassical regimes.

Background: Cavity Quantum Electrodynamics (CQED)

Excited Atoms in Resonant Cavities: Enhancement of Spontaneous Emission

We turn to CQED, which, (despite having roots in NMR) grew out of laser theory, as the study of atoms interacting with photons, inside a resonant cavity, tuned to the photon frequency, which is also that of the radiative transitions in question. The salient fact of CQED is that quantum emitters, be they atoms or spins, couple directly and strongly to the resonant cavity – or, in

the case of NMR, the tuned reception coil – thereby enhancing the rate of spontaneous emission, by several orders of magnitude. Recognition of this phenomenon, called cavity enhancement, is usually credited to Purcell,⁶ although B–P cite the later work of Suryan,⁷ whose arguments are based directly on NMR coils. Cavity enhancement can be large, exceeding 10 orders of magnitude, as we demonstrate in subsequent calculations. The magnitude of cavity enhancement is a key factor in generating NMR signals of observable strength. The converse effect – that detuning the cavity (or coil) inhibits spontaneous emission, is well known in NMR, and well documented.⁸

Since the relationship of NMR to CQED is a central motif throughout this article, we often use the term ‘cavity’ when referring to the NMR coil. (We may also, depending on circumstance, speak interchangeably of oscillators, resonators, and tuned inductors.)

Cavities and Radiation Oscillators

Preparatory to discussing quantum fields, we recall a simple example from classical physics, that is, the ripple tank – a device for producing and visualizing water waves, and a familiar fixture in undergraduate physics laboratories. The ripple tank employs a paddle, immersed in the water and harmonically driven, to excite waves, whose images are then viewed by projection on a screen. The point is elementary: namely, that a harmonic oscillator (the paddle) can source a classical wave.

This idea is taken over in quantum electrodynamics, which invokes the *radiation oscillator* – a virtual device, driving a given Fourier component of a quantum field, such as a particular mode of a resonant cavity. Then an array of virtual oscillators provides multimode excitation. An excited oscillator is deemed to be populated by photons; and its degree of excitation is measured by its occupation number, which counts the number of photons it contains.

Typically in quantum field theory, the radiation oscillator is constructed by quantizing a classical harmonic oscillator of unit mass; Dirac’s book,⁹ despite its legendary reputation for difficulty, is clear and simple on this point. Then in the quantum description of emission inside a laser cavity, a photon is transferred from an atom, to excite the radiation oscillator, whose occupation number increases by one. Concurrently, the atom drops from its excited to its ground state. The cavity field enters this description primarily as a factor in the coupling constant between atom and cavity.

Paradoxically, in the case of NMR, we shall have no need to invoke the abstraction of a virtual radiation oscillator – the LC oscillator comprising our NMR probe is a concrete object, whose features furnish the requirements for a quantum description. All that is needed is the quantization of the LC circuit, and this is achieved by analogy to a mechanical oscillator. A mechanical oscillator in classical physics – say, a pendulum – is described by the mass, the position, and the velocity of the plumb bob; the spring constant also enters the expression for Newton’s law. We substitute inductance for mass, charge for position, and current for velocity, as well as inverse capacitance for spring constant, to obtain, from Newton’s equation for the pendulum, no more nor

less than Kirchhoff’s equation for the LC oscillator. Inasmuch as a quantum treatment of the mechanical oscillator is possible, so it is for the LC oscillator. This forms the basis for a quantum description of NMR, to which we presently turn our attention. Before doing so, we note that quantization of the LC oscillator’s near field is problematic,¹⁰ due to the presence of longitudinal components, and is not here attempted.

Classical Harmonic Oscillators

Before showing how to couple a quantized LC oscillator to a spin, we first discuss the physical meaning of certain key terms which appear in the coupling Hamiltonian. For simplicity, we first give the classical Hamiltonian function for a lossless (i.e., undamped) mechanical oscillator, with mass m , and spring constant $k = \omega_0^2 m$:

$$\mathcal{H}_1 = \frac{1}{2m}(p^2 + m^2\omega_0^2x^2) \quad (1)$$

The position and momentum are p and x . The classical Hamiltonian for a lossless LC oscillator is similar in appearance:

$$\mathcal{H}_2 = \frac{1}{2L}(\varphi^2 + L^2\omega_0^2q^2) \quad (2)$$

where we substitute inductance L for mass m ; also the charge q takes the place of position x , and flux $\varphi = L\dot{q}$ (inductance times current) that of momentum $p = m\dot{x}$. By a well-known equation, we have $L\omega_0^2 = 1/C$, so that the spring constant becomes inverse capacitance. Note that the oscillator resonant frequency, ω_0 , will also be Larmor frequency in our later discussion.

Ladder Operators for Cavities

Conversion of these Hamiltonians to quantum mechanical form requires the introduction of ladder operators for the quantized harmonic oscillator, which we accomplish, first, by noting that (owing to free commutation in classical dynamics) the classical Hamiltonian \mathcal{H}_1 can be written as $1/2m$ times the product of $p + im\omega_0q$ (having dimensions of momentum) and its complex conjugate, $p - im\omega_0q$. Replacement of the conjugate variables p and q by the corresponding quantum operators (denoted by circumflex) and dividing by the quantity $\sqrt{2m\hbar\omega_0}$ yields the dimensionless ladder operators

$$\hat{a}^\dagger = (\hat{p} + im\omega_0\hat{q})/\sqrt{2m\hbar\omega_0} \quad (3)$$

$$\hat{a} = (\hat{p} - im\omega_0\hat{q})/\sqrt{2m\hbar\omega_0} \quad (4)$$

We here follow Dirac’s convention for the placement and signs of imaginary quantities; elsewhere, these operators are often written $i\hat{a}^\dagger$ and $-i\hat{a}$. Corresponding operators for the LC oscillator are gotten by the substitutions that convert between equations (1) and (2):

$$\hat{a}^\dagger = (\hat{\varphi} + iL\omega_0\hat{q})/\sqrt{2L\hbar\omega_0} \quad (5)$$

$$\hat{a} = (\hat{\varphi} - iL\omega_0\hat{q})/\sqrt{2L\hbar\omega_0} \quad (6)$$

From these we obtain directly the expression for magnetic flux in the oscillator:

$$\hat{\varphi} = \sqrt{(L\hbar\omega_0/2)}(\hat{a}^\dagger + \hat{a}) \quad (7)$$

Their Relation to Ladder Operators for Spins

Photon Swapping and the Spin-exchange Hamiltonian. We exploit the parallel between \hat{a} and \hat{a}^\dagger , and the familiar ladder operators, \hat{I}_- and \hat{I}_+ , for spins, by examining the spin-exchange term (for a pair of spins 1/2, labeled 1 and 2) which appears in the dipole coupling Hamiltonian, as well as that for strong scalar coupling, $\hat{I}_+^{(1)}\hat{I}_-^{(2)} + \hat{I}_-^{(1)}\hat{I}_+^{(2)}$. This is called the flip-flop term, since, for a pair of oppositely directed spins, it inverts the values of the z component angular momentum. Inasmuch as the lifting of a spin, from its ground state to its excited state, occurs by absorption of a photon, the flip-flop process is just the exchange of a photon between spins. For different orientations of spins, the following examples are illustrative:

$$\hat{I}_+^{(1)}\hat{I}_-^{(2)}|\beta\alpha\rangle = |\alpha\beta\rangle; \quad \hat{I}_+^{(1)}\hat{I}_-^{(2)}|\alpha\alpha\rangle = 0; \quad \hat{I}_-^{(1)}\hat{I}_+^{(2)}|\alpha\beta\rangle = |\beta\alpha\rangle \quad (8)$$

Cavity Operators for Creation and Annihilation of a Photon. We begin by stating without proof that the ladder operators, \hat{a}^\dagger and \hat{a} , act as follows, upon states of the quantum oscillator:

$$\hat{a}^\dagger|n\rangle = \sqrt{n+1}|n+1\rangle; \quad \hat{a}|n\rangle = \sqrt{n}|n-1\rangle \quad (9)$$

Specifically, \hat{a}^\dagger , called the *creation* operator, lifts the occupation number by unity and multiplies the resulting ket by the scalar $\sqrt{n+1}$. The action of \hat{a} (the *annihilation* operator) follows from the second equation above.

The Exchange of a Photon between a Spin and a Cavity. We next write the operator portion of the Hamiltonian for exchange of a photon between a spin and an oscillator, by analogy to photon exchange between two spins:

$$(\hat{a}^\dagger\hat{I}_-^{(i)} + \hat{a}\hat{I}_+^{(i)})|n, \alpha\rangle = \sqrt{n+1}|n+1, \beta\rangle \quad (10)$$

That is, the initial state $|n, \alpha\rangle$, comprising a cavity with n photons, and a spin up, is converted into the state $|n+1, \beta\rangle$, with $n+1$ photons in the cavity, and the spin down. The spin emits a photon, which is captured by the cavity, whose occupation number increases by one. Only the term $\hat{a}^\dagger\hat{I}_-^{(i)}$ is responsible here; the other term, $\hat{a}\hat{I}_+^{(i)}$, simply zeros the spin state, in accord with its well-known rules of operation. We also write

$$(\hat{a}^\dagger\hat{I}_-^{(i)} + \hat{a}\hat{I}_+^{(i)})|n, \beta\rangle = \sqrt{n}|n-1, \alpha\rangle \quad (11)$$

to show the action of the term $\hat{a}\hat{I}_+^{(i)}$, with the capture of a photon from the cavity by the spin. Note that our choice of the intuitive operator pairings, $\hat{a}^\dagger\hat{I}_-^{(i)}$ and $\hat{a}\hat{I}_+^{(i)}$, corresponding to $|\alpha\rangle$ as the excited spin state, implies a negative gyromagnetic ratio, for example, for an electron. *This will be reversed in subsequent examples when we consider the proton spin.*

The Jaynes–Cummings Model and its Application to NMR

A Simple Hamiltonian

Having these preliminaries in hand, we proceed with the quantized oscillator and the Jaynes–Cummings Hamiltonian. For a complete description of the NMR experiment, we divide the Hamiltonian into three terms, two describing the nuclear spin and the RF coil in mutual isolation, and a third – a coupling term – which specifies their interaction; similar equations to ours, but for electron resonance, are found in Louisell's book.¹¹ In the first two terms, we set the Larmor frequency and the oscillator frequency both to the value ω_0 . The coil is presumed lossless; we also omit relaxation. For the energy of the spin we have the Zeeman Hamiltonian, and for the cavity, the product of occupation number n and the photon energy $\hbar\omega_0$:

$$\mathcal{H}_1 = -\hbar\omega_0\hat{I}_z \quad (12)$$

$$\mathcal{H}_2 = \hat{a}\hat{a}^\dagger\hbar\omega_0 = n\hbar\omega_0 \quad (13)$$

To write the interaction, we recall the operator for magnetic flux in the coil, from equation (7) above.

For the interaction, we assume that the coil is single-turn Helmholtz, its and approximate its magnetic field by the flux divided by twice the window aperture (in meters squared). Using the expression for flux from equation (7), this leads to

$$\mathcal{H}_3 = -\hbar\frac{\Omega_0}{2}(\hat{a} + \hat{a}^\dagger)(\hat{I}_+ + \hat{I}_-) \quad (14)$$

for the familiar interaction term $-\boldsymbol{\mu} \cdot \mathbf{B} = -\mu_x B_x$, with $\Omega_0 = \sqrt{\hbar\omega_0 L/2}/2\sigma$ where σ is the window aperture, and we assume an x -directed RF field, using the identity $\hat{I}_x = (\hat{I}_+ + \hat{I}_-)/2$.

The quantity Ω_0 is called the Rabi *fundamental* frequency; as discussed below, it sets the frequency of Rabi *oscillation* when a single spin is present in the cavity. It is also apparent from equation (14) that Ω_0 serves as the coupling constant between spins and cavity. Note that its dimensions, hertz, are the same as the familiar spin–spin coupling constant J .

Then the entire Hamiltonian for the spin and coil combination is the sum of terms $\mathcal{H}_1 + \mathcal{H}_2 + \mathcal{H}_3$; since the cavity is considered lossless, we omit any coupling to a heat reservoir. We then invoke, without proof, the quantum machinery for transformation to the interaction picture, transforming with the sum $\mathcal{H}_1 + \mathcal{H}_2$, which leaves us with only \mathcal{H}_3 remaining. The behavior of this term under transformation is now described.

The Jaynes–Cummings Approximation

Multiplying out the operators in equation (14) gives four distinct terms $-\hat{a}\hat{I}_-$, $\hat{a}^\dagger\hat{I}_+$, $\hat{a}\hat{I}_+$, and $\hat{a}^\dagger\hat{I}_-$, – of which two are the flip–flip terms introduced above, corresponding to emission of a photon by the spin and absorption by the cavity, or vice versa. These are zero-quantum terms, which conserve energy, and experience no alteration under the transformation to the interaction frame, provided that the cavity is tuned exactly to the Larmor frequency of the spin; in particular, they acquire zero-frequency shift. Useful discussions may be found in expositions of the theory of lasers.^{12,13}

The other two terms represent simultaneous emission or absorption by both atom and cavity; these are two-quantum terms, which do not conserve energy. Under transformation to the interaction frame, these terms become oscillatory at twice the Larmor frequency.^{11–13}

The Jaynes–Cummings approximation consists in discarding the two-quantum terms; in laser theory this is called the rotating wave approximation¹³ and is analogous to the common rotating frame transformation in magnetic resonance, in which zero frequency terms are kept and terms at twice Larmor discarded.

We now write the J–C Hamiltonian in matrix form for a single spin, coupled to a coil,

$$\mathcal{H}_3 = -\hbar\Omega_0/2(\hat{a}^\dagger\hat{I}_+ + \hat{a}\hat{I}_-) \quad (15)$$

$$= \begin{bmatrix} 0 & 0 & 0 \\ 0 & 0 & -\hbar\frac{\Omega_0}{2} \\ 0 & -\hbar\frac{\Omega_0}{2} & 0 \end{bmatrix}$$

where the basis vectors are indicated by kets above the matrix, corresponding to (i) spin and cavity both in their ground states, (ii) excited spin with cavity in its ground state, and (iii) spin in its ground state with excited cavity. Because of our interest in proton NMR, we have here chosen the gyromagnetic ratio positive; the excited spin state is $|\beta\rangle$, and we must pair \hat{a}^\dagger with \hat{I}_+ , and \hat{a} with \hat{I}_- .

The Propagator for the Jaynes–Cummings Hamiltonian

\mathcal{H}_3 is block diagonal, comprising two submatrices of dimensions 1×1 and 2×2 . The 2×2 submatrix is mathematically identical to the Pauli matrix σ_x multiplied by $-\hbar(\Omega_0/2)$; yet it operates not only upon the spin but the cavity as well. Since the block elements do not interact when the matrix is exponentiated, the Schrödinger equation for \mathcal{H}_3 can be solved exactly, to give the propagator or time evolution operator:

$$P = \exp\left(-\frac{i}{\hbar}\mathcal{H}_3t\right) = \begin{bmatrix} 1 & 0 & 0 \\ 0 & \cos\Omega_0t/2 & i\sin\Omega_0t/2 \\ 0 & i\sin\Omega_0t/2 & \cos\Omega_0t/2 \end{bmatrix} \quad (16)$$

The integrability of the Schrödinger equation sets the Jaynes–Cummings model apart from most quantum mechanical problems involving the interaction of radiation and matter, where exact solutions are not obtainable in closed form, and one must resort to perturbation theory.

Spontaneous Emission by an Inverted Spin, and Rabi Oscillation.

If we express our basis elements as column vectors,

$$|0, \alpha\rangle = \begin{bmatrix} 1 \\ 0 \\ 0 \end{bmatrix}; \quad |0, \beta\rangle = \begin{bmatrix} 0 \\ 1 \\ 0 \end{bmatrix}; \quad |1, \alpha\rangle = \begin{bmatrix} 0 \\ 0 \\ 1 \end{bmatrix} \quad (17)$$

we can evolve the system, starting from a condition of the spin excited:

$$\exp\left(-\frac{i}{\hbar}\mathcal{H}_3t\right)|0, \beta\rangle = \cos\frac{\Omega_0t}{2}|0, \beta\rangle + i\sin\frac{\Omega_0t}{2}|1, \alpha\rangle \quad (18)$$

This equation resembles that for rotation of a spin 1/2 about the x axis¹⁴, but it describes not a rotation, rather a concerted transition of the spin and cavity – called *vacuum Rabi oscillation* –¹⁵ in which a state comprising an excited spin inside a cavity in its ground state transforms to a state comprising a spin in its ground state inside an excited cavity. (The term ‘vacuum’ ensures that there is no external injection of a RF field and will be dropped in the sequel.) This process is an example of spontaneous emission – pure quantum behavior, not described by the classical Bloch equations, which predict, absent relaxation, that an inverted spin does not evolve. To reinforce the point, we now show explicitly, by density matrix, that no transverse magnetization develops in this scenario.

The Same Example Treated by Density Matrix; Reduced Density Matrices. For a single spin inverted, and cavity in its ground state, the density operator is simply the outer product $|0, \beta\rangle\langle 0, \beta|$, written in matrix form as

$$\rho^{(\text{init})} = \begin{bmatrix} 0 & 0 & 0 \\ 0 & 1 & 0 \\ 0 & 0 & 0 \end{bmatrix} \quad (19)$$

Evolving this with the propagator P of equation (16) according to $\rho(t) = P(t)\rho(0)P^{-1}(t)$, and using the abbreviations $s = \sin(1/2)\Omega_0t$ and $c = \cos(1/2)\Omega_0t$, leads to

$$\rho(t) = \begin{bmatrix} 0 & 0 & 0 \\ 0 & c^2 & -isc \\ 0 & isc & s^2 \end{bmatrix} \quad (20)$$

(This is essentially the solution of an appropriate Liouville equation for the spin and cavity.) To separate the behavior of the spin from that of the cavity, we calculate the reduced density matrices¹⁶ – that for the spin obtained by tracing $\rho(t)$ over the cavity variables, and that for the cavity by tracing over the spins. For example, given a density matrix describing two particles, the general element is written $\langle n, m' | \rho | k, l' \rangle$ where the indices of one particle are primed and the other unprimed. For a generic element of the unprimed particle, we have $\langle n | \rho | m \rangle = \sum_{k'} \langle nk' | \rho | mk' \rangle$. Likewise, for the primed particle $\langle k' | \rho | l' \rangle = \sum_n \langle nk' | \rho | nl' \rangle$. Carrying this out for equation (20) gives

$$\rho^{(\text{spin})}(t) = \begin{bmatrix} s^2 & 0 \\ 0 & c^2 \end{bmatrix} \quad (21)$$

where $\rho_{11}^{(\text{spin})} = \langle \alpha | \rho^{(\text{spin})} | \alpha \rangle$, and so on. For clarity we give details of the calculation, with reference to equation (20) and to the ordering of states in equation (15):

$$\langle \alpha | \rho^{(\text{spin})} | \alpha \rangle = \langle \alpha, 0 | \rho | \alpha, 0 \rangle + \langle \alpha, 1 | \rho | \alpha, 1 \rangle = 0 + s^2 \quad (22)$$

$$\langle \beta | \rho^{(\text{spin})} | \beta \rangle = \langle \beta, 0 | \rho | \beta, 0 \rangle = c^2 \quad (23)$$

In a similar manner, the off-diagonal elements, corresponding to spin coherence, are shown to vanish, since, for example $\langle \beta, 0 | \rho | \alpha, 0 \rangle = 0$ and the term $\langle \beta, 1 | \rho | \alpha, 1 \rangle$ simply does not appear in the density matrix of equation (21).

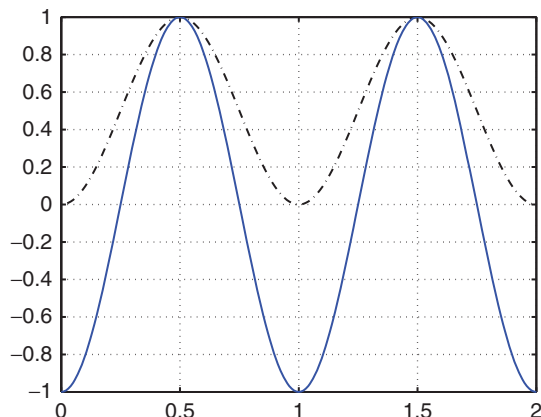


Figure 1. Evolution of a longitudinal magnetization due to a single spin in a lossless cavity, following inversion. A single spin is initially inverted and returns to its equilibrium orientation directly by spontaneous emission. The magnetization remains longitudinal throughout; no transverse moment develops. The solid trace shows the z -component (longitudinal) magnetization as a function of time; the dotted trace shows the oscillator occupation number. The horizontal axis (time) is denominated in units of the Rabi fundamental period

A similar calculation for the cavity yields

$$\rho^{(\text{cavity})}(t) = \begin{bmatrix} c^2 & 0 \\ 0 & s^2 \end{bmatrix} \quad (24)$$

Again, note the absence of coherence. The general expression for the mean cavity occupation number is $N = \sum_{n=1}^N (n-1)\rho_{nn}^{(\text{cavity})}$; in the case at hand, this reduces simply to $\rho_{22}^{(\text{cavity})}$ for the number of photons. However, the presence of a photon here does not imply the existence of an oscillatory field, which requires for its existence a coherent superposition of cavity states, as will appear in examples below.

Further Illustration of Rabi Oscillation/Nutation. To further illustrate Rabi oscillation (also called Rabi nutation), we calculate the expectation value of the z -component magnetization $M_z = \gamma\hbar\langle\hat{I}_z\rangle$, with $\langle\hat{I}_z\rangle = \text{tr}\rho^{(\text{spin})}(t)\hat{I}_z$.

Expanding the squared trigonometric terms in equation (21) as $1/2(1 \pm \cos \Omega_0 t)$ yields directly $\gamma\hbar\langle\hat{I}_z\rangle = -((1/2)\gamma\hbar)\cos \Omega_0 t$, where the negative sign accounts for the fact that we start with the spin in the state $|\beta\rangle$. Then our future labor is greatly simplified by renormalizing the constants so that the amplitude of the magnetization is simply the number of spins, yielding in this instance $M_z = -\cos \Omega_0 t$.

Figure 1 shows the longitudinal magnetization (blue trace), and the cavity occupation number (dotted black), for two periods of the Rabi fundamental frequency.

The spin, initially excited, gradually returns to its ground state by spontaneous emission of a photon – with the fractional values of occupation number representing appropriate linear superpositions of the states $|0, \beta\rangle$ and $|1, \alpha\rangle$ – finally arriving at the occupation number $n=1$. The cavity, now fully excited, then reexcites the spin, gradually transferring the photon back to it, to rearrive at occupation number $n=0$; the system has now completed one full period of Rabi nutation.

The entire process then recommences, and, in the absence of any loss mechanism, continues indefinitely, beyond the two Rabi periods we have shown. That there are no transverse components of magnetization (i.e., coherences), and no losses, means that we may picture a z -directed vector undergoing a repetitive process of shrinkage and regrowth, as it passes from negative to positive values, and back again. Since the classical Bloch equations, with relaxation omitted, predict a Bloch vector of constant length, this is an example of nonclassical behavior.

The Rabi Fundamental Frequency and Cavity Enhancement

We have already noted that Ω_0 not only determines the rate of Rabi oscillation but is also the coupling constant between spins and cavity. We must therefore know its magnitude if we are to assess the degree of cavity-enhanced spontaneous emission.

Cavity enhancement was introduced in our opening paragraphs. Qualitatively, it may be viewed as a manifestation of the greater oscillatory field strength produced by a photon inside a resonant cavity, relative to that of a photon in free space. Confining the photon to a cavity concentrates its energy in a small volume, increasing the local field strength per photon, which also serves to measure the coupling constant between atom and cavity. The stronger the coupling, the faster the rate of spontaneous emission – ergo cavity enhancement. In the case of NMR, of course, we have not a cavity but an LC oscillator. The field is nonetheless concentrated in the vicinity of the inductor, so we anticipate significant enhancement, which we measure by comparing the Rabi frequency in the coil with the rate of spontaneous emission in free space.

To calculate a numerical value of Ω_0 , we choose a static polarizing field strength of 14.1 T, that is, a proton Larmor frequency of 600 MHz. We next specify a reasonable Helmholtz coil, of a single turn, with round windows of diameter 1.27 cm, giving a measured inductance L of 77 nH. Using the definition given above, following equation (14), this leads to a value $\Omega_0 = 1.31 \times 10^{-4} \text{ s}^{-1}$ corresponding to an inverse emission period (for spin inversion in the Rabi cycle) of $4.17 \times 10^{-5} \text{ s}^{-1}$. Comparing this to the inverse lifetime for spontaneous emission of an isolated spin in free space at 14.1 T – $\mu_0\hbar\gamma^2\omega^3/\pi c^3 = 6 \times 10^{-21} \text{ s}^{-1}$, we find a difference, that is, a cavity enhancement, of an astonishing sixteen orders of magnitude. Jaynes and Cummings found a cavity of enhancement of $\sim 10^7$ for the ammonia maser. We attribute our larger enhancement to the small size of our coil relative to that of their cavity, leading to a relatively higher concentration electromagnetic flux per photon.

Radiation Damping: J–C Evolution of a Spin in the Transverse Plane

With this much preparation, we now embark upon the direct study of radiation damping, starting with a density matrix calculation for the initial condition of a spin tipped by $\pi/2$ about the y axis of a rotating coordinate frame. Since a spin inversion corresponds to absorption of an entire photon, a tip angle of $\pi/2$ appears to represent the absorption of half a photon – a physical impossibility. In fact, the photon state will always be a

linear superposition of the cavity ground and first excited states, weighted so that the mean occupation number never exceeds 1/2. The starting density matrix is

$$\rho^{(\text{init})} = 1/2 \begin{bmatrix} 1 & -1 & 0 \\ -1 & 1 & 0 \\ 0 & 0 & 0 \end{bmatrix} \quad (25)$$

with the elements ordered as in equation (15). The matrix in equation (25) can also be written as the direct product $|0\rangle\langle 0|$ with the sum of (minus) the Pauli matrix σ_x plus the identity matrix of dimension two. In contrast to our earlier example, we have spin coherence at the outset, which will give rise to cavity coherence, in a process recognizably analogous to classical radiation damping.

The density matrix, following evolution through time interval t , is

$$\rho(t) = 1/2 \begin{bmatrix} 1 & -c & is \\ -c & c^2 & -isc \\ -is & isc & s^2 \end{bmatrix} \quad (26)$$

leading to the reduced density matrices

$$\rho^{(\text{spin})}(t) = 1/2 \begin{bmatrix} 1 + s^2 & -c \\ -c & c^2 \end{bmatrix} \quad (27)$$

and

$$\rho^{(\text{cavity})}(t) = 1/2 \begin{bmatrix} 1 + c^2 & is \\ -is & s^2 \end{bmatrix} \quad (28)$$

Figure 2 shows the temporal evolution from equations (27) and (28); the solid green and blue traces give, respectively, the transverse and longitudinal magnetizations, M_x and M_z ; the dotted blue trace is the cavity one-quantum coherence, and the dotted black, the photon occupation number; the duration is two periods of the Rabi fundamental. The motion of the Bloch vector remains nonclassical, with the longitudinal magnetization evolving at the Rabi frequency and the transverse at half that value.

Since the energy of the spins is proportional to *negative* M_z , the growth of M_z and the corresponding diminution of M_x represent the flow of Zeeman energy – and the photon – from spin to cavity. This coincides with the growth of cavity coherence and the photon occupation number, both of which achieve their maximum amplitudes when M_x is zero, at which point (so to speak) half a photon is captured by the cavity. It is seen that spin coherence and cavity coherence exchange with each other directly, that is, one reaches achieves its maximum amplitude when the other reaches zero. Although we have nowhere invoked Faraday's law of induction, this exchange of coherences is seen to parallel the appearance of the induced RF field in an NMR coil, in the classical description of radiation damping.⁵ The transfer of Zeeman energy also parallels that in the classical description.

However, according to customary notions, any process designated as damping must embody some intrinsic dissipation; this is absent in our quantum description, since we have explicitly omitted the resistance of the coil. How can quantum mechanics describe radiation damping in a lossless coil? To resolve this dilemma, we must slightly expand our conception of damping and assert that the critical process is exactly the

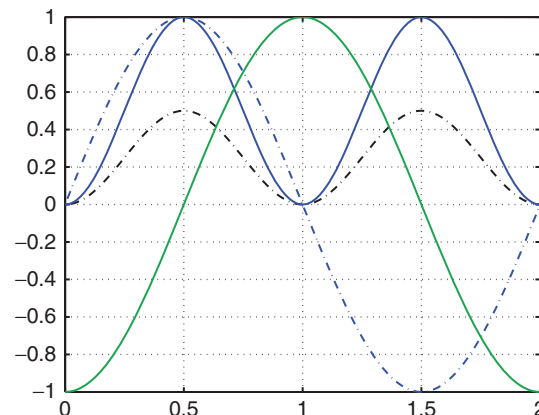


Figure 2. Prototypical radiation damping for a single spin in a lossless cavity: the evolution of transverse and longitudinal magnetizations, following an initial rotation of $\pi/2$. The solid green trace is M_x (transverse), the solid blue M_z (longitudinal). The dotted traces show the cavity one-quantum coherence (blue) and the cavity occupation number (black). The horizontal axis (time) is the same as in Figure 1, in units of the Rabi fundamental period

transfer of a photon from spin to coil, and that the subsequent fate of the photon is of secondary importance. Pursuing this line of thought, we invoke the Wigner–Weisskopf theory of spectroscopic linewidth¹⁷: the key factor is the rate of emission of a photon by an atom, not the evolution of the photon once emitted. In fact, we have elsewhere shown² that cavity losses can be included in a quantum model; for now, their absence simply means that emission is followed by reabsorption, in an endless cycle.

Adding More Spins to the Calculation

Our calculations so far are for a single spin; but the Jaynes–Cumplings Hamiltonian is straightforwardly modified¹⁸ to accommodate multiple spins, by a simple summation, as follows:

$$\mathcal{H}_3 = -\hbar \frac{\Omega_0}{2} \sum_{j=1}^N (\hat{a}^\dagger \hat{I}_+^{(j)} + \hat{a} \hat{I}_-^{(j)}) \quad (29)$$

Analytic solution is no longer straightforward, but numerical results are readily gotten; and the similarity, noted above, between quantum and classical models of radiation damping, obtains as well for multiple spins, as illustrated, for example, in Figure 3. This shows, for two spins, the transfer of Zeeman energy, via spin coherence, from the precessing magnetization to the tuned cavity, with the concomitant appearance of an induced oscillatory field, manifest as magnetic flux.

The transverse magnetization M_x is shown in green; the net cavity one-quantum coherence (to be discussed below) is given in dashed blue. The dashed black trace gives the expectation value of induced magnetic flux in the coil, normalized to the square root of the occupation number. Naturally, the time course of flux directly tracks that of the induced magnetic field. Since the transverse moment oscillates at one half the Rabi frequency, and since the cavity is assumed lossless, the zero of transverse moment coincides with the maximum induced

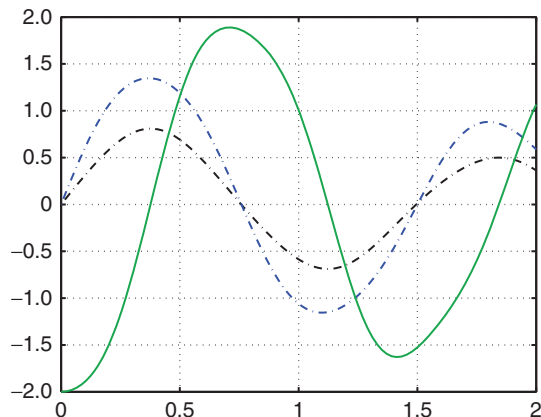


Figure 3. Radiation damping for a pair of spins in a lossless cavity: the evolution of transverse magnetization and cavity coherence and magnetic flux, following an initial rotation of $\pi/2$. The solid green trace is M_x (transverse), the dotted blue trace is the cavity one-quantum coherence; the black trace is the magnetic flux induced in the cavity. Time axis as in Figures 1 and 2. (Reproduced with permission from J. Tropp, J. Chem. Phys., 2013, 139, 014105-1. Copyright 2013, AIP Publishing LLC)

field; this matches the result in Figure 2, where the zero of M_x occurs at peak occupation number. Overall, Figure 3 illustrates once more the dynamics of NMR transduction, particularly the conversion of spin coherence to cavity coherence, about which we have remarked above, as well as the transfer of Zeeman energy from the spins to cavity, to create an oscillatory field. These processes together constitute the essential elements of radiation damping.

Buildup of Cavity Coherence with Multiple Spins. More details of the interaction of multiple spins with a cavity may be gotten; for example, the detailed development of one-quantum cavity coherence is shown in Figure 4.

When multiple spins are present, several coherences of the type $\rho_{n,n+1}^{(\text{cavity})}$ are formed sequentially in time; for instance, in the case of five spins, we have $\rho_{12}^{(\text{cavity})}$, $\rho_{23}^{(\text{cavity})}$, on up to $\rho_{56}^{(\text{cavity})}$. This temporal evolution is illustrated in the figure, with the coherences of ascending indices (solid traces) labeled with the color sequence navy, red, green, violet, cerulean (for $\rho_{12}^{(\text{cavity})}$, $\rho_{23}^{(\text{cavity})}$, etc.). A simple summation of these yields the dashed navy trace, roughly approximating a sinusoid; a summation weighted by the square roots of the occupation numbers gives the dashed black trace, closer to sinusoidal form, and representing the induced magnetic flux in the coil.

We have already noted, in our discussion of Figure 2, that mutual exchange of spin and cavity one-quantum coherences is characteristic of the process of radiation damping. Then since spin coherence, has, for a single-spin species, an invariable sinusoidal dependence upon time, the net cavity coherence must have a similar dependence. The calculations shown in Figure 4 demonstrate, for multiple spins, the complexity of cavity behavior, in which many individual coherences, of seemingly arbitrary form, combine to form a sinusoid.

In fact, a simpler version of this process holds for the results in Figure 3, where the net sinusoidal cavity coherence is in

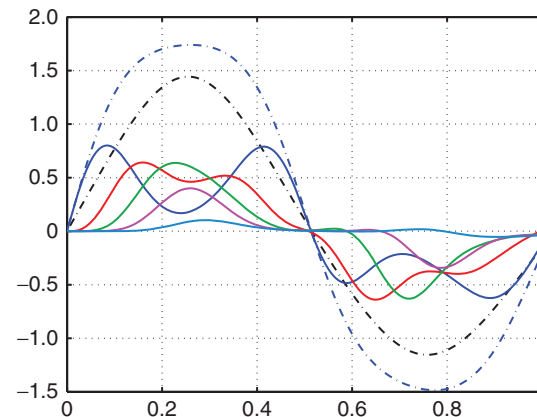


Figure 4. Evolution of cavity one-quantum coherence for five spins in a lossless cavity, following initial rotation of $\pi/2$. Individual coherences of the type $\rho_{n,n+1}^{(\text{cavity})}$, for $n = 1$ to $n = 5$. Further details given in text. The color scheme, for increasing n , is navy, red, green, violet, cerulean. The dotted blue trace is the direct summation of the individual coherences; the dotted black trace is the weighted summation representing the induced magnetic flux in the cavity/coil. Time axis as in previous figures. (Reproduced with permission from J. Tropp, J. Chem. Phys., 2013, 139, 014105-1. Copyright 2013, AIP Publishing LLC)

fact the resultant of two oddly shaped coherences, $\rho_{12}^{(\text{cavity})}$ and $\rho_{23}^{(\text{cavity})}$, which do not themselves appear in the figure.

Stimulated Emission from Multiple Spins. Figure 5 illustrates stimulated emission for increasing numbers of spins, initially tipped into the transverse plane. We plot the transverse magnetization against time for a single period of the Rabi fundamental, and take the position of the first zero crossing as a measure of the emission rate. Starting with two spins (solid blue trace), each successive curve represents addition of a single spin, ending at seven (dotted red trace).

The zero crossing occurs at progressively shorter times as more spins are added. To understand this, refer back to equation (29), and calculate the matrix element for emission of a single photon, from the cavity state $|n-1\rangle$ to $|n\rangle$ as:

$$\langle n | \mathcal{H}_3 | n-1 \rangle = \hbar \frac{\Omega_0}{2} \sqrt{n} \quad (30)$$

The enhancement factor \sqrt{n} is well known in quantum field theory, as the marker of stimulated emission, when $n > 1$.¹⁹ Strictly speaking, a *single* spin undergoing Rabi nutation in the presence of a cavity field comprising $n-1$ photons, will experience this enhancement, giving a Rabi frequency of $\Omega_n = \sqrt{n}\Omega_0$; but our situation, with *multiple* spins, is more complicated. Here, the value of n increases as each photon is emitted; this in turn increases the emission rate for succeeding photons. Despite the seeming complexity, a system with multiple spins undergoes an orderly process of Rabi oscillation, with more spins giving ever faster nutation, as is seen from the individual traces in the figure. Finally, it is worth noting in this context that a spin emitting into a cavity initially devoid of photons [$n=1$ in equation (30)], will evolve at the Rabi fundamental frequency, Ω_0 .

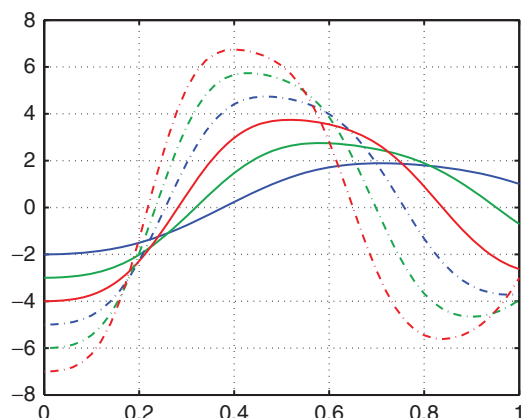


Figure 5. Stimulated emission for n spins, with $n=2$ to $n=7$, illustrated via transverse magnetization, following an initial rotation of $\pi/2$. The relative rapidity of emission is gauged by the first zero-crossing of the magnetization. The number of spins increases in color order blue, green, red, and from solid to dotted trace. Further discussion is given in the text. Time axis is as in previous figures, except only a single Rabi period is shown. (Reproduced with permission from J. Tropp, J. Chem. Phys., 2013, 139, 014105-1. Copyright 2013, AIP Publishing LLC)

In fact, it is also shown²⁰ that for samples of n spins, with $n \gg 1$, the net moment will nutate with the enhancement factor \sqrt{n} , a fact we will utilize in later calculations. In light of this, it is interesting to compare the maximum and minimum times for the first zero crossing in the figure, at approximately $0.39/\Omega_0$ and $0.21/\Omega_0$. Their ratio is 1.86, which we compare to the ratio for the square roots of numbers of spins, $\sqrt{7/2} = 1.87$. Without arguing the significance of the numerical agreement, it is clear that more spins mean faster emission – a direct result of stimulated emission. We later show that the enhancement in realistic NMR samples may amount to several orders of magnitude.

Quantum Mechanics and Radiation Damping

We have now established sufficient quantum basics to take up the question of radiation damping; but this will also require a brief review and revision of the classical theory.

Classical Radiation Damping, without the Filling Factor

A revised classical theory is given here as a necessary prelude to a quantum mechanical calculation. In the usual theory of radiation damping, a filling factor (so called) is introduced, to write Faraday's law for an NMR sample that does not completely fill the detection coil. Unfortunately, the literature gives multiple definitions of filling factor, many of them mutually incompatible, and none admitting of routine measurement. We therefore eliminate it, using the results of reciprocity theory^{21,22} to write the radiation damping constant in terms of the coil efficiency – essentially a measure of the power needed to nutate the magnetization, in a specified time, through an angle π . The discussion of power will also require that we abandon the notion of a lossless coil and introduce resistance, although within the context of a classical coil.

We begin with an initial magnetization M_0 , which has been tilted through an angle ϑ , to give longitudinal and transverse

components $M_0 \cos \vartheta$ and $M_0 \sin \vartheta$; we write the equation describing the balance of Zeeman energy E_z , as the spins (occupying a volume V) dissipate power in the coil's resistance (unspecified as yet) and tilt back toward the vertical:

$$\frac{dE_z}{dt} = M_0 V B_0 \sin \vartheta \frac{d\vartheta}{dt} \quad (31)$$

Then for a sample within a region of uniform B_1 field, the electromotive force, denoted ε , induced in the coil by Larmor precession, is the product of the Larmor frequency, the B_1 field per unit current, the sample magnetization, and the volume,²¹ with the imaginary factor i to provide the correct phase relationship

$$\varepsilon = i\omega_0 B_1(1) V M_0 \sin \vartheta \quad (32)$$

The Larmor frequency is ω_0 and the transverse magnetization M_T is given by $M_0 \sin \vartheta$, where ϑ is the tip angle. The sign of the imaginary can be positive or negative, depending on the choice made for the time factor in Maxwell's equations. Then since the intrinsic resistance R of the detection coil is effectively doubled by impedance matching the coil to its feed line,²³ the net power dissipated in the coil is $(1/2)\varepsilon^2/2R$, where the factor $1/2$ gives the rms value. Equating this with $-dE_z/dt$ (power is positive, but the energy is decreasing) leads to

$$\frac{-dE_z}{dt} = -M_0 V B_0 \sin \vartheta \frac{d\vartheta}{dt} = \frac{\{\omega_0 M_0 \sin \vartheta V B_1(1)\}^2}{4R} \quad (33)$$

or, for small tip angles ($\sin \vartheta \approx \vartheta$), straightforwardly to

$$\begin{aligned} \frac{d\vartheta}{dt} &= -k\vartheta \\ k &= \gamma\omega_0 M_0 V \zeta^2 / 4 \end{aligned} \quad (34)$$

where k is the radiation damping constant and we have introduced the symbol $\zeta = B_1(1)/\sqrt{R}$ for the efficiency of the coil, first given by Hoult and Lauterbur.²⁴ This is also equal to the total linear B_1 (not a rotating component) produced per unit of power absorbed by the probe, and, as such, is readily measured by determining the power needed for a π pulse. Note also that for $\vartheta = 0$, we have $\dot{\vartheta} = -k$.

Although equation (33) now contains R explicitly, it is important that equation (31) can nonetheless be used without knowing the resistance, provided only that we supply a value of the nutation rate $\dot{\vartheta}$.

Incidentally, with the definitions we have given, the damping constant may be written as a product of the factors: the (classical) nutation rate per unit current present in the coil – $\gamma B_1(I)/2I$ – and a current – $\omega_0 V M_0 B_1(I)/2IR$, equal in this case to the emf of the sample divided by the total resistance of the coil (intrinsic plus that from external load, coupled by impedance matching).

Stimulated Emission and Total Signal Power

We use equation (31), for the balance the Zeeman energy, to calculate the NMR signal power in various scenarios, using always the same reference sample – neat water – but varying the nutation frequency according to diverse assumptions. This enables the comparison of spontaneous and stimulated emission, without the necessity of solving the Liouville equation for a lossy

coil.² As noted at the outset, in our introductory paragraph, the change in Zeeman energy comprises both the radiated power, and that lost in the coil's own resistance; these are equal on the assumption of correct impedance matching.

We start with the formula for the magnetic dipole moment of a water sample.

$$\mu = M_0 V = \frac{1}{2} \gamma \hbar N M_w (\tanh \hbar \omega_0 / 2kT) \pi r^2 h_w \times 10^{-3} \quad (35)$$

where N is the Avogadro number, M_w is the molarity of water protons (110), r is the inside radius (in centimeter) of a 5 mm Wilmad™ NMR tube determined from the manufacturer's outer diameter and wall thickness (0.43 mm), and h_w is the height of the model probe window, 1.27 cm. The value at $T = 298$ K is 7.72×10^{-9} A m². The multiplicative factor of 10^{-3} converts the volume to liters, as required by the use of molarity. The Larmor frequency is 600 MHz.

We use an experimental value²³ for the coil efficiency ζ , corresponding to a pulse width of 6.8 μ s at 21.4 W absorbed by the probe: $\zeta = B_1 / \sqrt{2P_{\text{rms}}}$, where the power is doubled, since the definition of efficiency specifies peak current, whereas the measured power (e.g., from a spectrum analyzer) is typically rms. We get $\zeta = 2.64 \times 10^{-4}$ T/ $\sqrt{\text{watt}}$. From the efficiency and dipole moment, we calculate the radiation damping constant in equation (34): $k = 136$.

Also, using the inductance of our model Helmholtz coil and a coil quality (Q) factor of 200, when impedance matched (i.e., source loaded), the calculated coil resistance is 0.726Ω , which we will make use of presently.

Since the NMR signal⁵ has been historically considered to arise from coherent spontaneous emission, we first calculate the power for this case, in which the nutation rate is simply the Rabi fundamental frequency, which applies (cf equation (30) and discussion) when the cavity contains no photons at the outset; Heitler gives a clear discussion of this point.¹⁹ From equation (31), utilizing $\mu = M_0 V$ with $\vartheta = 0$ and $\dot{\vartheta} = \Omega_0$, the total dissipated power is 14.2 pW. Since the calculation is made, not for individual spins emitting independently but for the aggregate magnetization, we have an example of *coherent* spontaneous emission.^{5,25}

To calculate the peak power in radiation damping, we again utilize equation (31), but with the nutation rate given by the radiation damping constant, that is, $\vartheta = 0$, and $\dot{\vartheta} = -k$. This maximizes the total dissipated power, at 14.8 μ W.

We then argue that the increased power seen here – a full six orders of magnitude greater than that for coherent spontaneous emission, – arises from stimulated emission. (Stimulated emission does not require the active application of an external field, but only the presence of photons in the cavity.) We therefore need the number of photons in the energized coil, which is gotten from the energy equation of the inductor:

$$\frac{1}{2} LI^2 = n \hbar \omega_0 \quad (36)$$

with the maximum current I obtained from the emf (equation (32)) divided by twice the coil resistance (2×0.726 ohms = 1.45 ohms), since the voltage operates into the source-loaded coil. The result is 5.7 mA, leading to $n = 3.13 \times 10^{12}$.

Then recalling that $\Omega_n = \sqrt{n} \Omega_0$, and using $\sqrt{n} = 1.77 \times 10^6$, the enhanced value of dissipation, $\mu B_0 \Omega_n$, is calculated to be 20.0 μ W.

This result, although entirely quantum theoretic, lies well within 30% of the 14.8 μ W, calculated from the measured coil efficiency. We assert on this basis that quantum mechanics offers adequate explanation, from first principles, of signal strength in NMR.

New Perspectives in NMR Reception

A Magnetic Resonance and Quantum Optics

The Bloch equations (together with their descendants, the optical Bloch equations) have reliably described both NMR and quantum optics during half a century; as such, they are emblematic of the close relation between the two disciplines. The present work also reaffirms that kinship, showing how CQED can be used to explain the fine details of signal formation and reception in NMR.

In fact, the first application of the Jaynes–Cummings model to magnetic resonance was the proposal²⁶ for magnetic resonance force microscopy (MRFM), wherein it was shown theoretically how to couple a mechanical oscillator – a force microscopy cantilever with a magnetic tip – to a single spin. The coupling Hamiltonian was shown to be bilinear in ladder operators for both spin and oscillator, so that with minor modification, an electrical resonator could be substituted for the mechanical. Thus, the genesis of the approach given here.

The current work also challenges a proposition long held – that the strength of the NMR signal derives from coherent spontaneous emission.⁵ We have presented calculations which (we believe) make an unmistakable case for the essential role of stimulated emission. This is not done lightly, and we believe that additional justification can be sought in further discussion of the phenomenon of cavity enhancement.

Differing Views of Cavity Enhancement

The founding document of CQED is Purcell's abstract on cavity enhancement⁶; yet, his theory of this effect, which has dominated the discussion of NMR reception for 60 years, differs markedly from that proposed later by Jaynes and Cummings,¹ which today constitutes the gold standard in quantum optics. We sketch a comparison – necessarily incomplete – of the two theories, with the goal of bringing the J–C model more into the purview of NMR practitioners. Let us enumerate some dichotomies.

Jaynes and Cummings start with quantization of the cavity field (we convert their electric fields to magnetic) and then write the interaction term, equivalent to our $-\boldsymbol{\mu} \cdot \mathbf{B}_1$ which couples a spin to the cavity. They discard from the coupling Hamiltonian those terms which do not conserve energy, and solve the resultant Schrödinger equation exactly, for arbitrary nutation angles (e. g., π). Since the cavity field per photon is much larger than that in free space, cavity enhancement is automatically obtained.

Purcell, on the other hand, starts with the perturbation expression for spontaneous emission of a spin in free space,

including the factor of the density of states, as dictated by the Fermi golden rule. Cavity enhancement is introduced by the expedient of replacing the free space density of states with the inverse spectral width of the cavity (in hertz), ω_0/Q , that is, the cavity resonance frequency divided by its quality factor, Q . Since Q contains the effective cavity resistance, its introduction automatically introduces cavity dissipation into the emission rate, which contravenes the usual quantum theory of a lossy cavity²⁷ in which the deterministic Hamiltonian for spin-cavity coupling is separated from the stochastic Hamiltonian for damping. In modern theory, the transition rates of these two are independent of each other, whereas in Purcell's method they are not. In any case, large nutations are not describable within the perturbation regime.

Purcell's theory was used by Bloembergen–Pound in their exposition of radiation damping in NMR, and is consequently well known. Bloembergen–Pound give a classical theory of large nutations, based on Bloch's equations; but their quantum treatment, referring back to Purcell, is restricted to small nutations. We believe that the method of Jaynes–Cummings deserves to be better known in the NMR community, due to its comparative directness, its ability to handle large tip angles, and its ongoing important role in quantum optics.

The Transition from Quantum to Classical Behavior

It is perhaps surprising that the Bloch equations are not readily derivable from the Jaynes–Cummings model, except under quite restrictive conditions.²⁸ This is because the Bloch operator describes an infinitesimal rotation of the spins, whereas the J–C Hamiltonian describes not a rotation, but a concerted transition of spins and cavity. This accounts, on the whole, for the instances of nonclassical behavior noted earlier. The imposition of a so-called coherent, or Glauber^{29,30} state for the cavity allows one to obtain the Bloch equations, since a Glauber state is an eigenfunction of the cavity ladder operators; but the emergence of a Glauber state, starting from Fock states of the cavity, is not theoretically understood. Therefore, the question of the transition from quantum to semiclassical, or classical behavior, must be considered as unresolved, in both magnetic resonance and in quantum optics.

Acknowledgment

Much of the work described here was supported by GE Healthcare Technologies, during the author's tenure there; the American Institute of Physics is also thanked for permission to reprint materials from figures which appeared in Journal of Chemical Physics.

Biographical Sketch

James S. Tropp (b 1947), BA in 1970 (New York University), PhD in 1976 (University of Chicago, P. B. Sigler advisor) Postdoctoral study at Brandeis University (A. G. Redfield advisor) and MIT (J. S. Waugh

advisor). Scientist and engineer for over 30 years in the NMR and MRI industries, specializing in hardware and NMR physics, at Nicolet Magnetics, GE NMR Instruments, Diansonics MRI, Toshiba America MRI, and GE Healthcare Technologies. Over 50 articles in peer-reviewed journals, upwards of a dozen patents.

Related Articles

Abragam, Anatole: 'The Bible'; Ramsey, Norman F.: Origins of Magnetic Resonance; Quantum Optics: Concepts of NMR

References

1. E. T. Jaynes and F. W. Cummings, *Proc. IEEE*, 1963, **51**, 89.
2. J. Tropp, *J. Chem. Phys.*, 2013, **139**, 014105-1.
3. J. Raimond, H. Brune, and S. Haroche, *Rev. Mod. Phys.*, 2001, **73**, 565.
4. R. H. Mabuchi and A. C. Doherty, *Science*, 2002, **298**, 1372.
5. N. Bloembergen and R. V. Pound, *Phys. Rev.*, 1954, **95**, 8.
6. E. M. Purcell, *Phys. Rev.*, 1946, **69**, 674, B10.
7. G. Suryan, *Curr. Sci.*, 1949, **18**, 203.
8. A. Abragam, *The Principles of Nuclear Magnetism*, Oxford University Press: London, 1961, 65.
9. P. A. M. Dirac, *The Principles of Quantum Mechanics*, 3rd edn, London: Oxford, 1947, Chap 6.
10. O. Keller, *Quantum Theory of Near-field Electrodynamics*, Springer-Verlag: Berlin, 2011, 17, Chap. 22.
11. W. H. Louisell, *Quantum Statistical Properties of Radiation*, Wiley: New York, 1990, 324.
12. M. Sargent III, M. O. Scully, and W. E. Lamb, *Laser Physics*, Addison Wesley: Reading, 1977, 230 ff.
13. H. Haken, *Laser Theory*, Springer Verlag: Berlin, 1970, 29.
14. A. Messiah, *Quantum Mechanics*, North-Holland Publishing Co.: Amsterdam, 1963, 546.
15. L. Allen and J. H. Eberly, 'Optical Resonance and Two-Level Atoms', Dover Publications, Inc., New York, 1987, Chap. 3.
16. F. W. Cummings, *Phys. Rev.*, 1965, **140**, A1051.
17. W. H. Louisell op. cit., p. 285 ff.
18. M. Tavis and F. W. Cummings, *Phys. Rev.*, 1968, **170**, 379.
19. W. Heitler, *The Quantum Theory of Radiation*, 3rd edn, Dover: New York, 1984, 178.
20. Y. Kaluzny, P. Goy, M. Gross, J. M. Raimond, and S. Haroche, *Phys. Rev. Lett.*, 1983, **51**, 1175.
21. D. I. Hoult and R. E. Richards, *J. Magn. Reson.*, 1976, **24**, 71.
22. J. Tropp, *Phys. Rev. A*, 2006, **74**, 062103.
23. J. Tropp and M. Van Criekinge, *J. Magn. Reson.*, 2010, **206**, 161.
24. D. I. Hoult and P. C. Lauterbur, *J. Magn. Reson.*, 1979, **34**, 425.
25. R. H. Dicke, *Phys. Rev.*, 1954, **93**, 99.
26. J. A. Sidles, *Phys. Rev. Lett.*, 1991, **68**, 1124.
27. P. R. Rice and H. J. Carmichael, *IEEE J. Quantum Electron.*, 1988, **24**, 1351.
28. P. L. Knight and P. W. Milonni, *Phys. Rep.*, 1981, **66**, 21.
29. R. J. Glauber, *Phys. Rev.*, 1963, **131**, 2766.
30. W. H. Louisell op. cit., p 104 ff.